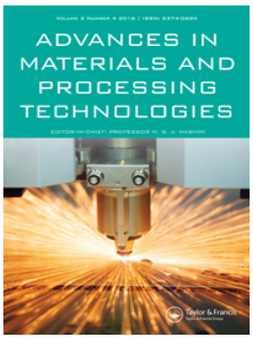

Advances in Materials and Processing Technologies

ISSN: 2374-068X (Print) 2374-0698 (Online) Journal homepage: www.tandfonline.com/journals/tmpt20

Surface properties and tribocorrosion behaviour of a thermal sprayed martensitic stainless steel coating after pulsed plasma nitriding process

Ferda Mindivan & Harun Mindivan

To cite this article: Ferda Mindivan & Harun Mindivan (2016) Surface properties and tribocorrosion behaviour of a thermal sprayed martensitic stainless steel coating after pulsed plasma nitriding process, Advances in Materials and Processing Technologies, 2:4, 514-526, DOI: 10.1080/2374068X.2016.1247232

To link to this article: https://doi.org/10.1080/2374068X.2016.1247232

ADVANCES IN MATERIALS AND PROCESSING TECHNOLOGIES, 2016
VOL. 2, NO. 4, 514–526
http://dx.doi.org/10.1080/2374068X.2016.1247232

Taylor & Francis
Taylor & Francis Group

Surface properties and tribocorrosion behaviour of a thermal sprayed martensitic stainless steel coating after pulsed plasma nitriding process

Ferda Mindivan[a] and Harun Mindivan[b,c]

[a]Technical Programs Department, Bilecik S.E. University, Bilecik, Turkey; [b]Mechanical and Manufacturing Engineering Department, Bilecik S.E. University, Bilecik, Turkey; [c]Central Research Laboratory, Bilecik S.E. University, Bilecik, Turkey

ABSTRACT

In this work, the effects of pulsed plasma nitriding on HVOF-sprayed martensitic stainless steel coating were investigated. Martensitic stainless steel coating was pulsed plasma nitrided at 793 K under 0.00025 MPa pressure for 43200 s in a gas mixture of 75% N_2 and 25% H_2. The pulsed plasma nitriding resulted in not only an increase in the surface hardness, but also improvement of dry sliding wear and tribocorrosion resistance of the HVOF sprayed martensitic stainless steel coating because of the Cr, Fe_3, and Fe_4 N phases. However, the corrosion resistance of the HVOF-sprayed martensitic stainless steel decreased notably by nitriding process.

ARTICLE HISTORY
Accepted 8 October 2016

KEYWORDS
HVOF spray coating; pulsed plasma nitriding; stainless steel; wear; corrosion; tribocorrosion

1. Introduction

Thermally sprayed stainless steel coatings in use today to repair damaged components of turbine blades and valve parts against corrosion and wear are an economic solution.[1,2] Previous studies [1,3] showed that the presence of porosity and plenty of oxides in the sprayed stainless steel coatings can ease the penetration of aggressive media through the coating onto the interface between the coating and the substrate. Moreover, their comparatively low hardness and insufficient wear resistance are still the main slow down factors that limit an implementation of these coatings.[4,5]

Plasma nitriding is an effective thermochemical diffusion process that is widely used in order to enhance the surface hardness, wear and corrosion resistance of metals, especially stainless steels.[4–6] Several researchers have investigated the effect of plasma nitriding and nitrocarburising treatment on the surface hardness and load-bearing capacity of high-velocity oxygen fuel (HVOF)-sprayed stainless steel coatings.[7] However, there is no recent information about the dry sliding wear, corrosion and tribocorrosion performance of pulsed plasma nitrided HVOF-sprayed martensitic stainless steel coating. In the present study, HVOF-sprayed martensitic stainless steel coating has been subjected to the pulsed plasma

CONTACT Harun Mindivan harun.mindivan@bilecik.edu.tr

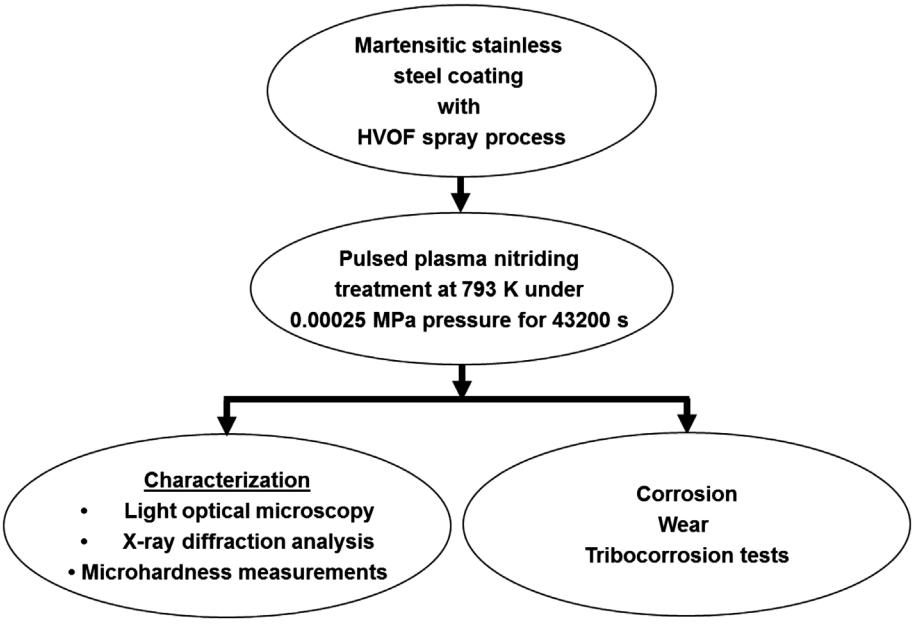

Figure 1. Schematic presentation of preparation and characterisation of coatings.

nitriding treatment with N_2–H_2 gas mixture, and then, its dry sliding wear, corrosion and tribocorrosion performance have been evaluated.

2. Experimental details

Steel plates were cut to the dimensions of 20 mm × 20 mm × 4 mm. Initially, the steel plates were coated with an intermediary Ni–Cr layer that increases the adhesion of coating. This was due to the fact that the Ni–Cr layer provided an overall increase in coating thickness and corrosion resistance in conjunction with enhanced fracture toughness.[8] The schematic presentation of preparation and characterisation of coatings is given in Figure 1. Martensitic stainless steel coatings were applied by HVOF thermal spray process on the steel plates. Before pulsed plasma nitriding, the surfaces of the HVOF-sprayed martensitic stainless steel coating were ground using 1200 grit SiC paper and mechanically polished with a fine grade Al_2O_3 paste to achieve a certain surface uniformity. Finally, the surfaces were thoroughly degreased with acetone and ultrasonically cleaned. The coatings were then pulsed plasma nitrided at 793 K under 0.00025 MPa pressure for 43200 s in an industrial furnace (Er-Mir Textile and Machine Ltd) in a gas mixture of 75% N_2 and 25% H_2. The coatings were cross sectioned and ground with successive SiC papers (grit 320–1200) and polished mechanically. They were then etched with 2% Nital, for metallographic examinations.

Microstructural characterisation of the coatings was made by microscopic examinations, X-ray diffraction (XRD) and microhardness measurements. Microscopic examinations were performed on the cross sections of the coatings by utilising Nikon Eclipse LV150 light optic microscope (LOM). XRD analysis was carried out by utilising CuK_α radiation with a Panalytical Empyrean diffractometer. The cross-sectional microhardness measurements

were carried out using a Vickers microhardness tester (Wolpert) with a load 50 g and a dwell time of 10 s.

The electrochemical tests were carried out using a Gamry model PC4/300 mA potentiostat/galvanostat controlled by a computer with DC 105 Corrosion analysis software in the corroding media of aerated solution of 3.5 wt.% NaCl at room temperature. Before potentiodynamic polarisation measurements, an initial delay of 45 min was employed in order to measure the open circuit potential (OCP) between working and reference electrodes. Potentiodynamic polarisation curves were generated by sweeping the potential from cathodic to anodic direction at a scan rate of 1 mVs^{-1}, starting from −1 up to +1 V. The corrosion tests were evaluated from the potentiodynamic polarisation. Finally, the surface images of the corroded coatings were examined using Zeiss Supra Field Emission Gun Scanning Electron Microscope (FEG-SEM) equipped with Energy Dispersive X-ray Spectroscopy (EDS) in order to determine the morphology of the developed corrosion.

Dry sliding wear tests of the coatings were performed on a reciprocating wear tester operating in ball-on-disc configuration at room temperature. In this configuration, an Al_2O_3 ball with a diameter of 10 mm was sliding forward and backward against the coatings with a sliding speed of 1.7 cm s^{-1}. Normal load of the test, sliding amplitude (wear track length) of the reciprocating motion and overall sliding distance were 5 N, 10 mm and 50 m, respectively. During the wear tests, the temperature and the relative humidity were maintained as 20 ± 5 °C and 30 ± 5%, respectively. The coefficient of friction (COF) was recorded automatically by the sensing cell mounted in the tester. Width and depth of the wear tracks were measured by a surface profilometer (Mitutoyo Surftest SJ-400) to calculate wear rate of the coatings. Following the wear tests, wear tracks were examined by a SEM.

Tribocorrosion tests were conducted in a triboelectrochemical cell containing 25 ml of 3.5 wt.% NaCl solution installed on a tribometer with the working surface of the coatings facing upwards against the counter material (10 mm diameter alumina ball). The tests were performed at OCP conditions. A potentiostat was used to record the potential between the coating and the reference electrode during tribocorrosion tests. The tribocorrosion tests consisted of the three steps: (1) stabilisation of the OCP for at least 10 min; (2) rubbing under the OCP for 45 min; (3) standby at the OCP after rubbing for 10 min. The sliding started in a reciprocating system with total stroke length of 10 mm, 1.7 cm s^{-1} sliding speed, normal load of 5 N and total sliding distance of 50 m. All corrosion and tribocorrosion tests were repeated at least three times in order to have repeatability. During the test, coating surface with an area of 1.5 cm^2 was exposed to the corrosive electrolyte. After tribocorrosion tests, the coatings and alumina balls were cleaned following the same cleaning procedure applied before testing and the contact surfaces of coatings and alumina balls were examined by SEM and LOM, respectively.

3. Results and discussion

Figure 2 shows the low and high magnification cross-sectional LOM micrographs of the pulsed plasma nitrided HVOF-sprayed martensitic stainless steel coating. The HVOF-sprayed martensitic stainless steel coating had a dense layer and tight bonding between the coating and substrate. The coating also possessed unmelted, resolidified splats and oxide veins.

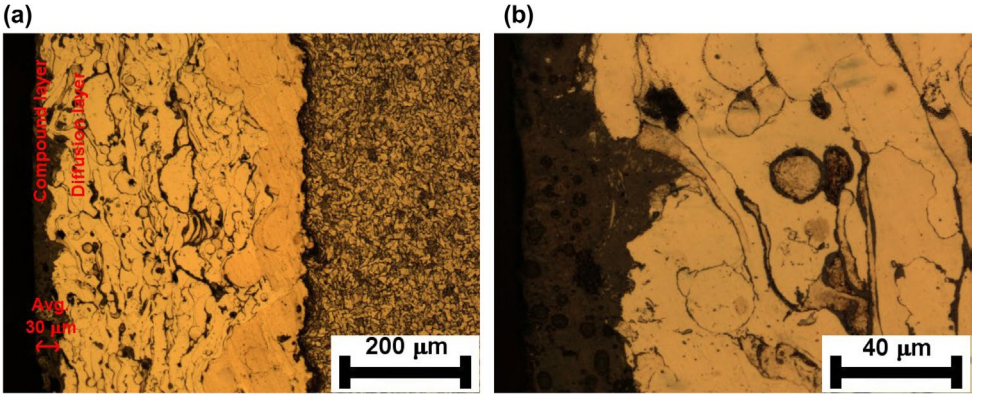

Figure 2. (a) Low and (b) high magnification cross-sectional LOM micrographs of the pulsed plasma nitrided HVOF-sprayed martensitic stainless steel coating.

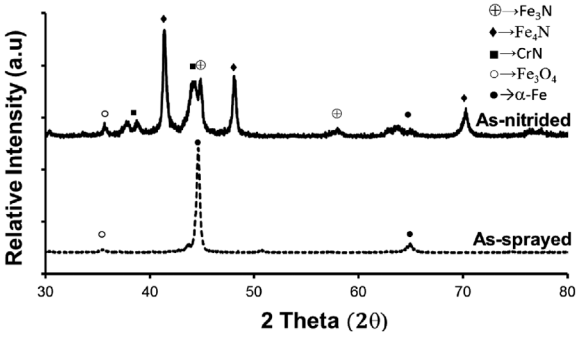

Figure 3. XRD patterns of the unnitrided and pulsed plasma nitrided HVOF-sprayed martensitic stainless steel coatings.

Pulsed plasma nitriding produced a layer with a thickness of about 30 µm on the surface of the HVOF-sprayed martensitic stainless steel coating, which had a BCC crystal structure. The cross-section morphology of pulsed plasma nitrided HVOF-sprayed martensitic stainless steel coating consisted of an outer compound zone and an inner diffusion zone. Generally, the compound zone contains nitrides formed from nitride-forming elements in the material.

The XRD examinations shown in Figure 3 demonstrate the transformation of the phases present in the unnitrided and pulsed plasma nitrided HVOF-sprayed martensitic stainless steel coatings. The results show that the dominant phases in the surface layer of the unnitrided HVOF-sprayed coating were α-Fe and Fe_3O_4. However, the pulsed plasma nitriding treatment induced new phases corresponding to Cr, Fe_3, and Fe_4 N peaks.

Figure 4 shows the cross-sectional microhardness values of the unnitrided and pulsed plasma nitrided HVOF-sprayed martensitic stainless steel coating layers. The maximum cross-sectional microhardness of the unnitrided coating was in the range of 260–320 $HV_{0.05}$. However, the surface microhardness of the coating subjected to nitriding was above 880 $HV_{0.05}$, three times greater than that of coating produced without nitriding. Pulsed plasma

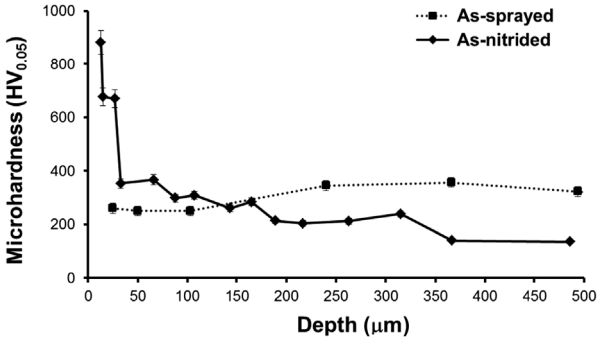

Figure 4. Cross-sectional microhardness variation of the coatings.

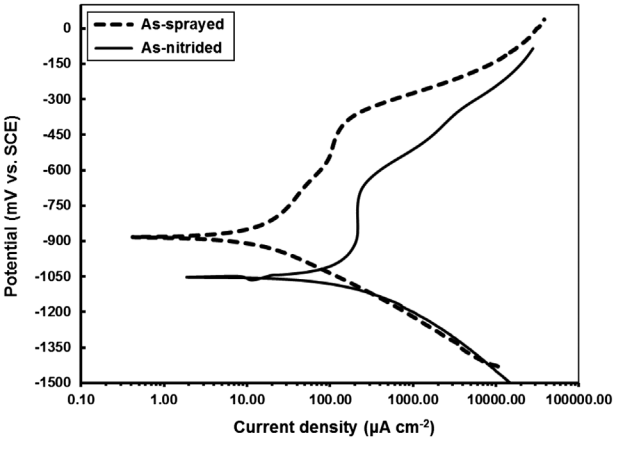

Figure 5. Potentiodynamic polarisation curves for the coatings.

nitrided coating maintained a high microhardness value above 880 $HV_{0.05}$ from the surface to a depth of ~15 μm due to the precipitation of Cr, Fe_3 and Fe_4 N in the compound layer and the microhardness decreased rapidly with the distance from the surface. The decrease in the microhardness on the case depth profile of the pulsed plasma nitrided coating can be attributed to the reduction of nitrogen concentration in the diffusion zone.[9]

Figure 5 presents the typical potentiodynamic polarisation curves for two coatings in a 3.5 wt.% NaCl solution. It can be seen that the pulsed plasma nitrided coating showed a much worse corrosion resistance than the unnitrided coating in terms of significantly reduced corrosion potential (from about −883 to −1050 mV vs. SCE) and increased corrosion current density (from about 23×10^{-6} to 120×10^{-6} A/cm^2). This observation indicates that the examined HVOF-sprayed martensitic stainless steel coating without nitriding had better corrosion protection for steel substrate.

The unnitrided coating surface seems less damaged (Figure 6(a)). On the other hand, on the nitrided surface, there is severe signature of corrosion attack, and hence, pits, which are observed on the surface after corrosion test, are more pronounced in the micrograph (Figure 6(b)). EDS analysis in a corroded area as depicted in Figure 6(b) indicates that

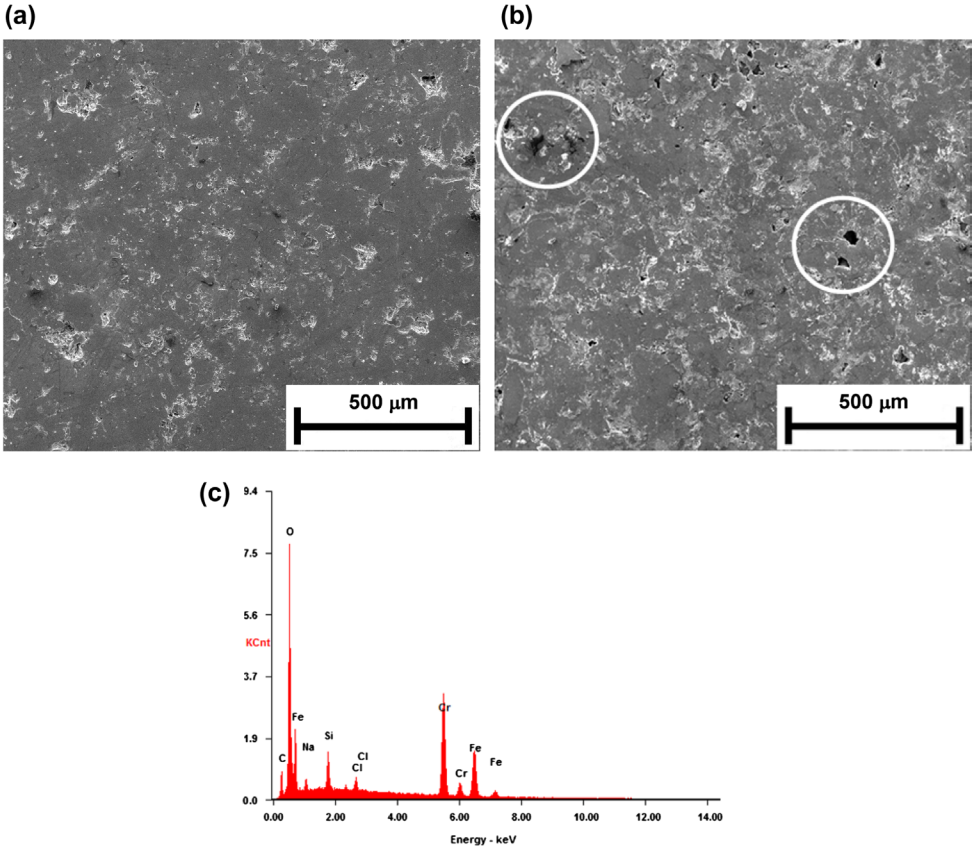

Figure 6. Corrosion surfaces of the (a) unnitrided, (b) nitrided coatings and (c) EDS analyses of corrosion products inside the corroded area indicated in circles.

Cr, Fe-based corrosion products are present (Figure 6(c)). Poor corrosion resistance of the nitrided coating is likely due to the precipitation of Cr N in the diffusion zone and the resulting depletion of chromium in solid solution.[6,10]

Figure 7 shows the results of the wear track appearances, cross-sectional profiles, wear rate and COF values of the coatings in the case of dry sliding. The unnitrided HVOF-sprayed martensitic stainless steel coating had high wear rate ($18.4 \times 10^{-5} \pm 0.5$ mm^3/Nm), as indicated by broadly surface damage and the depth of the wear track formed by Al_2O_3 ball. Since the HVOF-sprayed martensitic stainless coating was stacked with melted particles and hard oxide layers (Figure 2), the sprayed martensitic stainless steel coating used for this study exhibited lower wear rate than the bulk martensitic ones, which had very similar values ($125.8–133.9 \times 10^{-5}$ mm^3/Nm) as shown in Ref. [11]. On the nitrided coating surface with lower wear rate ($9.8 \times 10^{-5} \pm 2$ mm^3/Nm), very small or no wear track was formed when compared to the unnitrided coating surface. An average depth of 2 µm was obtained for the nitrided coating, whereas the unnitrided coating showed an average depth of 12 µm. Additionally, the unnitrided coating showed friction coefficient values in the range of 0.64–0.80 with relatively large fluctuations; however the friction coefficient of the nitrided coating reached a steady state value of about 0.62 with minor fluctuations. In

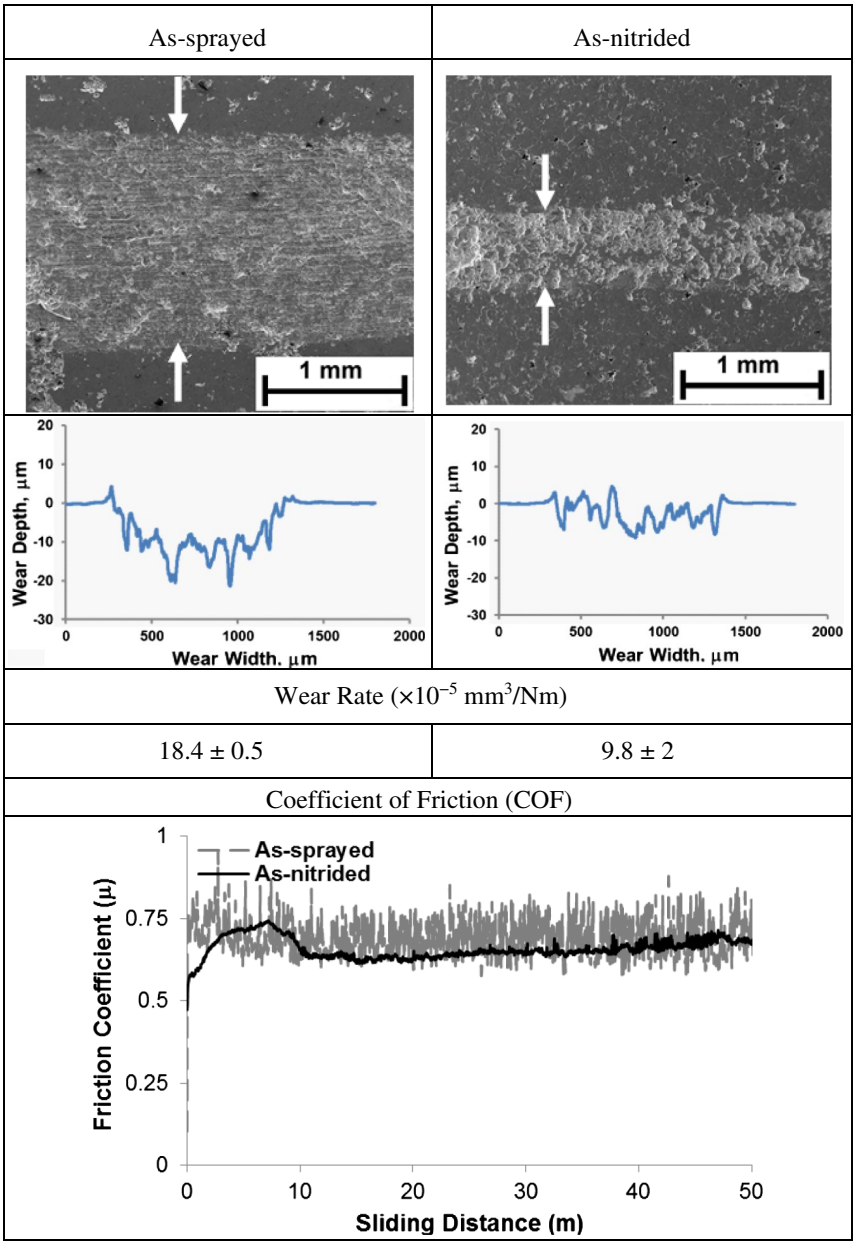

Figure 7. Dry sliding wear track appearances, cross-sectional profiles, wear rate and COF values of the examined coatings (Arrows indicate the wear tracks).

summary, the pulsed plasma-nitriding treatment effectively improved the wear resistance of the HVOF-sprayed martensitic stainless steel coating.

Figure 8 shows SEM micrographs of the worn surfaces of the unnitrided and nitrided HVOF-sprayed martensitic stainless steel coatings. It can be seen from the micrographs that, on the unnitrided surface the steel splats were flattened as a result of intense plastic deformation during wear. This micrograph also shows that some of the splat fragments

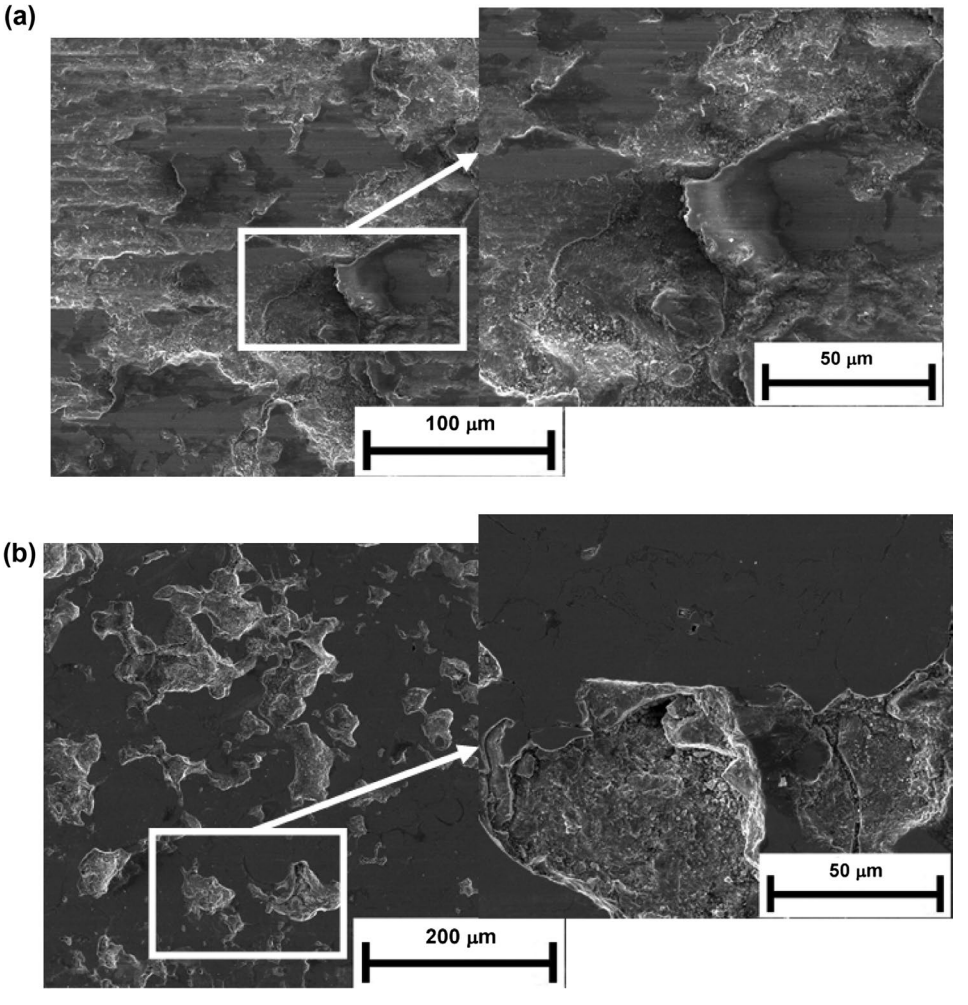

Figure 8. The worn surface topographies of the (a) unnitrided and (b) nitrided coatings.

were forged on contact surface by the Al_2O_3 ball. On the uneven surface of the nitrided coating, there is no indication of loss of splats; it still has capability to support the load of 5 N because of the ability of the nitrided layer to resist plastic deformation, as well as to eliminate adhesion between contact surfaces.

The evolution of the OCP with time before, during, and after the sliding is represented in Figure 9 for both coatings, together with the COF values recorded during the sliding. In the unnitrided coating, when sliding started, OCP values dropped down sharply, it means that the passive film becomes fully destroyed at a 5 N normal load. A galvanic coupling between the passive unworn surface (cathode) and the depassivated worn surface (anode) forms.[12,13] The longer sliding goes, the more area is active, the more negative OCP is Refs. [13–15]. Once the sliding is ended, the OCP starts to increase with a high speed and reaches the initial OCP back after some time. This indicates the re-establishment of passive state on the surface in the wear track. However, an opposite behaviour was observed for the as-nitrided coating. When sliding started, instead of decreasing, the OCP suddenly increases

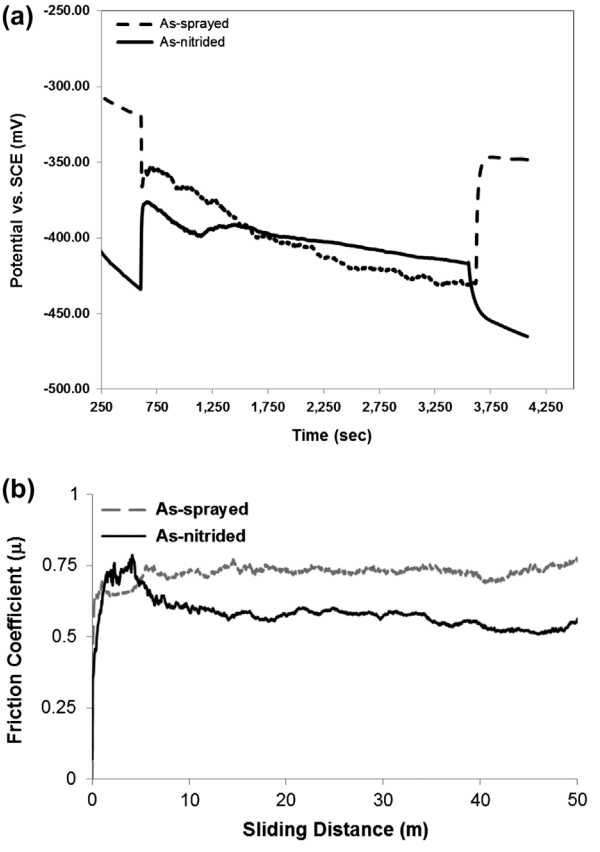

Figure 9. (a) OCP and (b) COF curves obtained during sliding.

and then decreases steadily until the end of the friction test. After the end of rubbing, there is a transitional decrease of the potential. Initial OCP after immersion of the unnitrided coating in the electrolyte and before the start of rubbing was more positive than in the case of nitrided coating. However, the OCP after the first half of sliding is higher for nitrided coating compared with unnitrided coating. It has been reported in the aforementioned study of Toptan et al. [16] that an increase on the OCP values of Al–B_4C composites in a 0.05 M NaCl solution was occurred due to the accumulated wear debris or tribolayer that acted as a protective layer. On the other hand, Figure 9(b) shows the evolution of the COF with sliding distance for both coatings. In this sense, unnitrided coating presents an average COF value of 0.75 ± 0.05, while the COF of the nitrided coating starts high and then decreases to a steady state value (0.54 ± 0.02) after about 4 m sliding distance. These differences in the COF could be related to a different contact area and wear–corrosion mechanism under the studied conditions. The common feature of the friction curves of the unnitrided HVOF-sprayed martensitic stainless steel coating under dry sliding conditions is heavy fluctuations throughout testing period (Figure 7). In order to clarify these differences, wear scar morphology generated after tribocorrosion tests was analysed by means of SEM (Figure 10).

In the case of unnitrided coating, a wide sliding track including abrasion scratches is observed along the sliding direction (Figure 10(a)). This could be attributed mainly to the

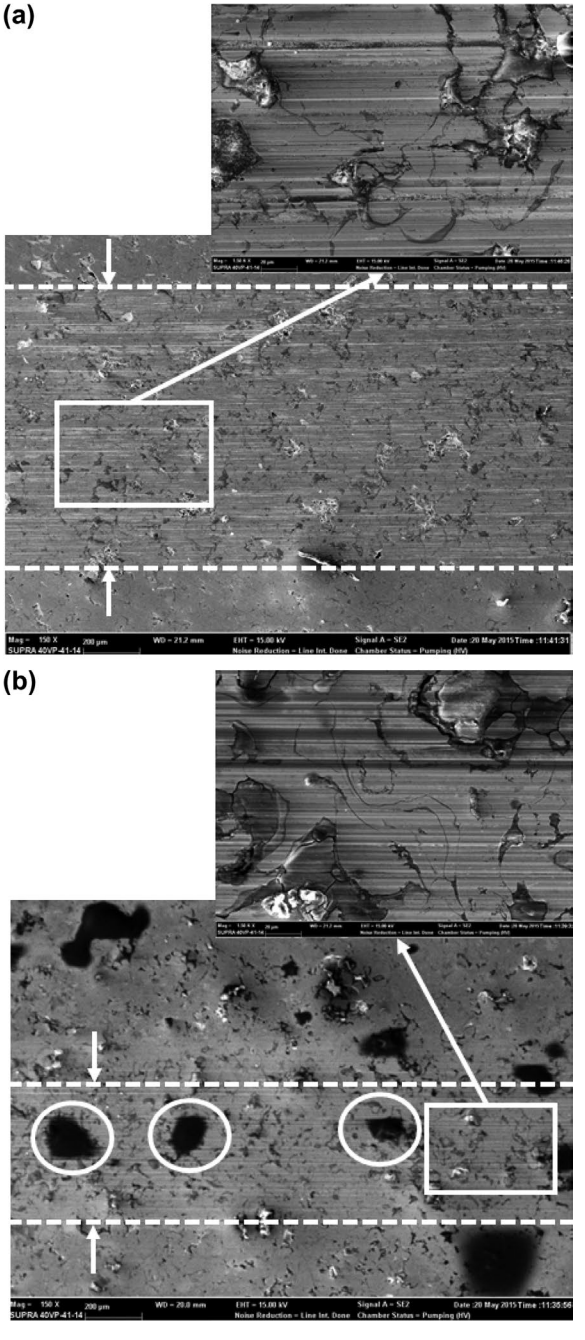

Figure 10. SEM images of the wear tracks of the (a) unnitrided and (b) nitrided coatings after tribocorrosion test.

dissolution of the coating due to the removal of the oxide surface film by the abrading action of the Al_2O_3 ball. As suggested by Berradja et al. [12] on tribocorrosion behaviour of stainless steels, the presence of a plastically dominated deformation induced by wear could reduce the capacity of restoration of the surface film, accelerate the dissolution of stainless

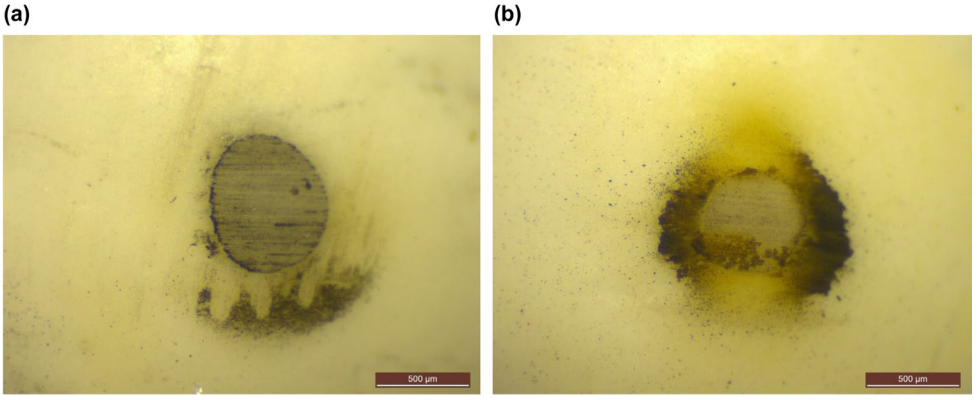

Figure 11. OM morphology on the Al_2O_3 counter parts for the (a) unnitrided and (b) nitrided coatings after tribocorrosion.

steel under tribocorrosion conditions. The degree of surface damage of worn surface significantly decreased with the pulsed plasma nitriding process (Figure 10(b)). Since the wear track of the nitrided coating having a higher OCP after 1450 s of sliding period was characterised by a relatively smooth appearance (Figure 10(b)) due to the higher hardness of the nitrided layer, less plastic flow and few fine scratches are induced in the wear track during sliding, thus the wear track is less activated than in the unnitrided coating. A less activated surface will result in higher OCP and will repassivate more quickly. Furthermore, a Fe-rich protective tribolayer, as revealed by EDS, was present on the nitrided surface by formation of black shaded areas indicated in circles (Figure 10(b)), and this is consistent with the results of variation of COF according to Figure 9(b).

The wear morphology of the Al_2O_3 counter parts was analysed by LOM (Figure 11). No transfer film on the Al_2O_3 ball for the unnitrided coating was observed (Figure 11(a)). However, a uniform and tenacious transfer film for the nitrided coating was formed (Figure 11(b)). The above analysis is consistent with the variation of the COF with sliding distance (Figure 9(b)). In addition, Figure 10 shows the SEM image of the nitrided surface, which indicated the presence of wear debris in comparison with the unnitrided coating.

4. Conclusion

Pulsed plasma nitriding treatment was performed on HVOF-sprayed martensitic stainless steel coating with a BCC structure. The coatings were characterised by microstructure analysis, microhardness measurements, corrosion, dry sliding wear and tribocorrosion tests, and the most relevant conclusions can be summarised as follows:

(1) The nitride layer on the HVOF-sprayed coating was composed of compound and diffusion layers.
(2) HVOF-sprayed martensitic stainless steel coating followed by pulsed plasma nitriding showed higher hardness, dry sliding wear and tribocorrosion resistance when compared to the coating without nitriding.

(3) The applied pulsed plasma nitriding process is not effective in improving the corrosion resistance of the HVOF-sprayed martensitic stainless steel coating in the potentiodynamic tests.

Acknowledgments

The financial support of the research foundation of Bilecik S.E. University (Project No.: 2015-01.BSEU.03-04) is gratefully acknowledged. The authors are grateful to the Central Research Laboratory and Mechanical and Manufacturing Engineering Department of Bilecik S.E. University for the technical support. We would also like to express our thanks to Dr Ersin. E. KORKMAZ for the support given in nitriding process.

Disclosure statement

No potential conflict of interest was reported by the authors.

Funding

This work was supported by the research foundation of Bilecik S.E. University [grant number 2015-01.BSEU.03-04].

ORCID

Ferda Mindivan http://orcid.org/0000-0002-6046-2456
Harun Mindivan http://orcid.org/0000-0003-3948-253X

References

[1] Suegama PH, Fugivara CS, Benedetti AV, et al. Electrochemical behavior of thermally sprayed stainless steel coatings in 3.4% NaCl solution. Corros Sci. 2005;47:605–620.
[2] Guilemany JM, Fernandez J, Espallargas N, et al. Influence of spraying parameters on the electrochemical behaviour of HVOF thermally sprayed stainless steel coatings in 3.4% NaCl. Surf Coat Tech. 2006;200:3064–3072.
[3] Zhao L, Lugscheider E. Influence of the spraying processes on the properties of 316L stainless steel coatings. Surf Coat Tech. 2002;162:6–10.
[4] Esfandiari M, Dong H. The corrosion and corrosion–wear behaviour of plasma nitride 17-4PH precipitation hardening stainless steel. Surf Coat Tech. 2007;202:466–4678.
[5] Adachi S, Ueda N. Formation of S-phase layer on plasma sprayed AISI 316L stainless steel coating by plasma nitriding at low temperature. Thin Solid Films. 2012;523:11–14.
[6] Li XY, Dong H. Effect of annealing on corrosion behaviour of nitrogen S phase in austenitic stainless steel. Mater Sci Tech. 2003;19:1427–1434.
[7] Park G, Bae G, Moon K, et al. Effect of plasma nitriding and nitrocarburizing on HVOF-sprayed stainless steel coatings. J Therm Spray Techn. 2013;22:1366–1373.
[8] Mindivan H. Wear behavior of plasma and HVOF sprayed WC-12Co+6% ETFE coatings on AA2024-T6 aluminum alloy. Surf Coat Tech. 2010;204:1870–1874.
[9] Mindivan F, Mindivan H. Comparisons of wear performance of hardened Inconel 600 by different nitriding processes. Procedia Eng. 2013;68:730–735.
[10] Bernardelli EA, Borges PC, Fontana LC, et al. Role of plasma nitriding temperature and time in the corrosion behaviour and microstructure evolution of 15-5 PH stainless steel. Kovove Mater. 2010;48:105–115.

[11] Dalmau A, Rmili W, Joly D, et al. Tribological behavior of new martensitic stainless steels using scratch and dry wear test. Tribol Lett. 2014;56:517–529.
[12] Berradja A, Bratu F, Benea L, et al. Effect of sliding wear on tribocorrosion behaviour of stainless steels in a Ringer's solution. Wear. 2006;261:987–993.
[13] Ponthiaux P, Wenger F, Drees D, et al. Electrochemical techniques for studying tribocorrosion processes. Wear. 2004;256:459–468.
[14] Azzia M, Paquette M, Szpunar JA, et al. Tribocorrosion behaviour of DLC-coated 316L stainless steel. Wear. 2009;267:860–866.
[15] Fernandes AC, Vaz F, Ariza E, et al. Tribocorrosion behaviour of plasma nitrided and plasma nitrided+oxidised Ti6Al4V alloy. Surf Coat Tech. 2006;200:6218–6224.
[16] Toptan F, Alves AC, Kerti I, et al. Corrosion and tribocorrosion behaviour of Al–Si–Cu–Mg alloy and its composites reinforced with B_4C particles in 0.05 M NaCl solution. Wear. 2013;306:27–35.